JOURNAL OF THERMOPHYSICS AND HEAT TRANSFER
Vol. 8, No. 2, April–June 1994

Evaluation of Simple Rate Expressions for Vibration-Dissociation Coupling

David A. Gonzales* and Philip L. Varghese†
University of Texas at Austin, Austin, Texas 78712

We consider relatively simple expressions for inelastic state-to-state and state-specific dissociative rate coefficients for use in vibrational master equation studies of shock-heated CO, N_2, and O_2 highly dilute in Ar. Rotationally averaged inelastic rate coefficients are determined using information theory. Rotationally averaged dissociative rate coefficients are computed using an expression we developed earlier and refined in this work. The master equation is linearized by neglecting diatom-diatom collisions and recombination. This allows us to use efficient eigenvector-eigenvalue matrix techniques. We show that the information theoretic rate coefficients are easily formulated and more accurate than commonly used Schwartz, Slawsky, and Herzfeld rate coefficients; they are therefore well suited for engineering solutions of the master equation. Our master equation results indicate that the most significant contribution to dissociation comes from low- and midlying vibrational levels. In addition, we find that the omission of multiquantum transitions results in significant underpredictions of the average vibrational energy and average dissociative rate coefficient.

Introduction

VIBRATION-DISSOCIATION coupling has been examined recently by several researchers[1–4] and also by us.[5–7] Here we continue our studies and evaluate relatively simple expressions for inelastic (bound) state-to- (bound) state rate coefficients and state-specific dissociative rate coefficients. We seek expressions which are more accurate than those derived from first-order theories and which are well suited for engineering solutions of the vibrational master equation.

We limit our study to shock-heated mixtures of diatomic gases highly dilute in an argon heat bath. We neglect diatom-diatom collisions and consider only the dissociative reaction (i.e., no recombination). These assumptions result in linear vibration-dissociation kinetics and a vibrational master equation which may be solved using efficient eigenvector-eigenvalue matrix techniques. We simulate shock heating by instantaneously raising the heat bath temperature to some final constant value. We then compute the time evolution of the vibrational populations from an initial equilibrium distribution to the steady-state condition. The inelastic and dissociative rate coefficients we compute are rotationally averaged. We assume a Boltzmann distribution of rotational states at the bath gas temperature, and thus we solve a system which is in rotational equilibrium throughout the vibrational relaxation process.

We have chosen the simpler linear problem for several reasons. First, there are experimental and computational data available to calibrate and verify the inelastic and dissociative rate coefficients for dilute mixtures. Second, the full linear problem (i.e., an analysis including all state-to-state transitions) can be solved in a matter of 3–5 CPU s on a Cray Y-MP, making the linear problem extremely affordable. Third, we expect to extrapolate lessons learned in these studies to facilitate future solutions of the nonlinear problem in which diatom-diatom collisions and back reactions (recombination) are included.

Computations were performed on p-H_2 to compare our results with those obtained using more sophisticated and expensive techniques. The other diatomic molecules considered in this article are CO, N_2, and O_2.

Inelastic State-to-State Rate Coefficients

In previous papers[5,6] we discussed multistate methods to compute inelastic state-to-state rate coefficients $k(v \to v')$ and state-specific dissociative rate coefficients $k(v \to c)$, where v and v' are initial and final vibrational quantum numbers, respectively, and where c denotes the continuum of dissociated (product) states. However, the multistate method, while more accurate than first-order theories,[5] remains an inefficient means to compute thousands of rate coefficients required for master equation calculations, even with the acceleration schemes we discussed.[6]

The inelastic rate coefficients used in this work are computed using the information theoretic approach of Procaccia and Levine.[8] In this section we will only briefly discuss information theory and refer the interested reader to the literature for a more comprehensive description.[8,9]

The rotationally averaged rate coefficients $k(v \to v'; T)$, where T is the translational-rotational temperature, may be written in terms of the surprisal $I(v, v'; T)$:

$$I(v, v'; T) \equiv -\ln [k(v \to v'; T)/k^0(v \to v'; T)] \quad (1a)$$

$$= \lambda_0 + \lambda |E_v - E_{v'}|/\kappa T \quad (1b)$$

where Eq. (1b) assumes a linear surprisal. Here, E_v is the vibrational energy of level v; λ_0 and λ are parameters discussed below; and κ is the Boltzmann constant. Equation (1b) is the so-called exponential gap form for $I(v, v'; T)$ [and hence for $k(v \to v'; T)$]. The rate coefficient $k^0(v \to v'; T)$ is the "prior" rate coefficient and is given by

$$k^0(v \to v; T) = \sum_j Y_j(v|T) \sum_{j'} g_s(j') k^0(vj \to v'j'; T) \quad (2)$$

Presented as Paper 93-0481 at the AIAA 31st Aerospace Sciences Meeting, Reno, NV, Jan. 11–14, 1993; received Feb. 1, 1993; revision received June 2, 1993; accepted for publication June 14, 1993.

*Graduate Student, Department of Aerospace Engineering and Engineering Mechanics; currently Assistant Professor, Department of Aeronautics and Astronautics, Massachusetts Institute of Technology, Cambridge, MA 02139. Member AIAA.

†Associate Professor, Department of Aerospace Engineering and Engineering Mechanics. Senior Member AIAA.

where

$$Y_j(v|T) = [Q_{\text{rot}}(v; T)]^{-1} g_s(j)(2j + 1)\exp(-E_{vj}/\kappa T) \quad (3)$$

$$Q_{\text{rot}}(v; T) = \sum_{j=j_{\min}}^{j_{\max}(v)} g_s(j)(2j + 1)\exp(-E_{vj}/\kappa T) \quad (4)$$

$$k^0(vj \rightarrow v'j'; T) = RC(T)(2j' + 1)\Delta \exp(\Delta)K_1(\Delta) \quad (5)$$

$$\Delta = (E_{vj} - E_{v'j'})/2\kappa T \quad (6)$$

The prior rate represents the rate one would expect in the absence of any dynamical bias in the collision process. The surprisal is thus a measure of the deviation of the actual rate coefficient from the prior rate. In many cases, the surprisal has been observed[8,9] to vary linearly with the energy defect $|E_v - E_{v'}|/\kappa T$.

In Eqs. (2–6), $Y_j(v|T)$ is the equilibrium fraction of molecules in the state (v, j); $Q_{\text{rot}}(v; T)$ is the partition function of the rotational manifold associated with level v; j is a rotational quantum number; and $g_s(j)$ is the nuclear spin degeneracy. Because CO is heteronuclear, nuclear spin degeneracy may be neglected. One can set $g_s = 1$ for all j and j', and the sums over j and j' are unrestricted. The most abundant isotopes of N_2 and O_2 are homonuclear ($^{14}N_2$ and $^{16}O_2$), so nuclear spin statistics must be considered. For N_2, in the ground electronic state ($^1\Sigma_g^+$), $g_s = 6$ for even j and $g_s = 3$ for odd j. Thus, the sums in Eqs. (2) and (4) are split into separate sums over even and odd j, respectively, each with an appropriate spin degeneracy. It should also be noted that the allowed transitions in Eq. (2) are from even j to even j' and from odd j to odd j'. This is because collisions do not change the nuclear spin symmetry. For O_2 in its ground (degenerate) electronic state ($^3\Sigma_g^-$), $g_s = 0$ for even j and $g_s = 1$ for odd j. Therefore, only odd j values need be considered in the sums. The energies E_{vj} are determined by a nonlinear least squares fit to solutions of the radial Schrödinger equation using the ground electronic state internuclear potential of Huxley and Murrell.[10] We computed 79, 59, and 44 bound vibrational levels for the rotationless state of CO, N_2, and O_2, respectively. The temperature dependent term $C(T)$ and the proportionality constant R are provided for completeness, but, as will be shown below, cancel out when computing $k(v \rightarrow v'; T)$. $K_1(\Delta)$ is the first-order modified Bessel function of the second kind. The upper triangular elements of the prior rate coefficient matrix $K^0_{v'v} = k^0(v \rightarrow v'; T)$ were computed first using Eq. (2), and the remainder were determined using detailed balance. (Reversing this order gave unsatisfactory numerical results, as might be expected, because the lower triangular section contains the comparatively small excitation rates).

The utility of the information theoretic approach is its ability to generate or "synthesize" all the (bound) state-to- (bound) state transition rate coefficients $k(v \rightarrow v'; T)$ in a direct manner.[8] To synthesize, the rate coefficients are first written as

$$k(v \rightarrow v'; T) = A(T)k^0(v \rightarrow v'; T)\exp(-\lambda|E_v - E_{v'}|/\kappa T) \quad (7)$$

where it can be shown[8] that

$$A(T) = \exp(-\lambda_0) = k(v \rightarrow v; T)/k^0(v \rightarrow v; T) \quad (8)$$

Equation (8) involves only the elastic rates (i.e., $|E_v - E_{v'}| = 0$). The rotationally averaged elastic prior rate coefficient is

$$k^0(v \rightarrow v; T) = RC(T) \sum_{j=j_{\min}}^{j_{\max}(v)} Y_j(v|T) \times \sum_{j'=j_{\min}}^{j_{\max}(v)} g_s(j')(2j' + 1)\Delta \exp(\Delta)K_1(\Delta) \quad (9)$$

where $j_{\min}$ and $j_{\max}(v)$ are common lower and upper bounds, respectively. Using Eq. (9) in Eq. (8) implies $A(T) \propto [RC(T)]^{-1}$, and Eq. (5) implies $k^0(v \rightarrow v'; T) \propto RC(T)$. Thus, Eq. (7) is independent of $RC(T)$ and may be rewritten as

$$k(v \rightarrow v'; T) = \hat{A}(T)\hat{k}^0(v \rightarrow v'; T)\exp(-\lambda|E_v - E_{v'}|/\kappa T) \quad (10)$$

where

$$\hat{k}^0(v \rightarrow v'; T) = \sum_j Y_j(v|T) \sum_{j'} g_s(j')(2j' + 1)\Delta \exp(\Delta)K_1(\Delta) \quad (11)$$

$$\hat{A}(T) = k(v \rightarrow v; T) \left[\sum_{j'=j_{\min}}^{j_{\max}(v)} Y_j(v|T) \times \sum_{j'=j_{\min}}^{j_{\max}(v)} g_s(j')(2j' + 1)\Delta \exp(\Delta)K_1(\Delta) \right]^{-1} \quad (12)$$

As explained below, we need not compute the right side of Eq. (12), and only present it for completeness. [Equations (9), (11), and (12) of Ref. 11 are incorrect but do not affect the results presented therein. The corresponding equations of this article give the correct expressions.] The surprisal parameter λ is obtained by requiring that the rate coefficients [Eq. (10)] obey the sum rule[8,9]

$$\Gamma(v; T) \equiv \sum_{v'} (E_{v'} - E_v)k(v \rightarrow v'; T) \quad (13a)$$

$$= \frac{V(\infty) - E_v}{(p\tau)/\kappa T} \quad (13b)$$

where $V(\infty)$ and $(p\tau)$ represent average quantities of the bulk system of relaxing oscillators. $V(\infty)$ is the average vibrational energy at equilibrium, and $(p\tau)$ is the product of the pressure p and the vibrational relaxation time τ. This product is computed by the formula of Millikan and White.[12] Given that $V(t)$ is the average vibrational energy of the bulk system at time t, Eq. (13) is a necessary and sufficient condition for the (assumed) exponential relaxation of $V(t)$ to its equilibrium value $V(\infty)$.[8] Thus, Eq. (13) relates the microscopic rates $k(v \rightarrow v'; T)$ to the macroscopic observable $V(t)$.

By forming the ratio $\Gamma(1; T)/\Gamma(0; T)$, $(p\tau)/\kappa T$, and $\hat{A}(T)$ cancel, and λ is obtained by iteration. Once λ is determined, the value for $\hat{A}(T)$ is computed using Eq. (13) with $v = 1$. Hence, it is not necessary to compute the right side of Eq. (12). Equation (10) inherently satisfies detailed balance because it is symmetric in E_v and $E_{v'}$, and (as discussed above) the prior rates satisfy detailed balance.

Note that an entire set of rate coefficients can be easily generated by knowing only the energies E_{vj} and the product $(p\tau)$. One does not require information about potential energy surfaces, inverse range parameters, etc.

State-Specific Dissociative Rate Coefficients

In this work, we use an expression for the state-specific dissociative rate coefficient $k(v \rightarrow c; T)$ that we have developed and present in detail elsewhere.[13] In our model, dissociation proceeds from all vibrational-rotational states for which $E_{vj} \leq D_0$, where D_0 is the dissociation energy of the diatom (i.e., we neglect dissociation from quasibound states).

The v-dependent dissociative rate coefficient is

$$k(v \rightarrow c; T) = \sum_{j=j_{\min}}^{j_{\max}(v)} Y_j(v|T)k(vj \rightarrow c; T) \quad (14)$$

where the internal-state-dependent rate coefficient is given by

$$k(vj \rightarrow c;\ T) = \varepsilon(v)Z\left(\frac{x_p + \Delta_d}{x_{p_{\max}} + \Delta_{d_{\max}}}\right)^{1/2} \times \exp[-(\Delta_d - \Delta_{d_{\max}})]\exp[-\lambda_D(\Delta_d - \Delta_{d_{\max}})] \quad (15)$$

Here, $\Delta_d = \beta(D_0 - E_{vj})$; $\Delta_{d\max} = \beta(D_0 - E_{vj\max})$; $\beta = 1/\kappa T$; x_p and $x_{p\max}$ are variables which arise from thermal-averaging approximations; $Z = \sigma_{HS}(8\kappa T/\pi\mu)^{1/2}$; and $\sigma_{HS} = \pi(d_i + d_{Ar})^2/4$. Z is the hard sphere rate coefficient, σ_{HS} is the hard sphere cross section, and d_i and d_{Ar} are the effective diameters[14] of the diatom i and the Ar atom, respectively. The reduced mass of the diatom-Ar pair is μ. The surprisal (or "bias") parameter for dissociation is λ_D. This parameter is assumed to be temperature independent and is to be determined. Once λ_D is obtained, $k(vj \rightarrow c;\ T)$ and $k(v \rightarrow c;\ T)$ are completely specified.

The "bridging function" $\varepsilon(v)$ is given by

$$\varepsilon(v) = \varepsilon_{quad}(v) = (1 - \sigma_0/\sigma_{HS})(v/v_{max})^2 + \sigma_0/\sigma_{HS} \quad (16a)$$

or

$$\varepsilon(v) = \varepsilon_{exp}(v) = \left(\frac{1 - \sigma_0/\sigma_{HS}}{1 - e^{-1}}\right)[1 - \exp(-v/v_{max})] + \sigma_0/\sigma_{HS} \quad (16b)$$

σ_0 is the cross section for dissociative transitions from state ($v = 0, j = j_{max}$). The product $\varepsilon(v)Z$ represents the maximum value for $k(vj \rightarrow c;\ T)$ for dissociative transitions from a given v. We make the prescription that when $E_{vj} = E_{vj\max} \approx D_0$, then $k(vj \rightarrow c;\ T) \rightarrow k(vj_{max} \rightarrow c;\ T) = \varepsilon(v)Z$. This biases the dissociative rate coefficients to high-lying internal states and is the unique feature of our model.

The results of Haug et al.[15] indicate that those molecules with internal energy $E_{vj} \approx D_0$ and with high vibrational quantum number have relatively higher dissociative cross sections. This implies that vibrational energy is more effective than rotational energy in causing dissociation when $E_{vj} \approx D_0$. We have developed the bridging function $\varepsilon(v)$ to account for this observation. $\varepsilon(v)$ approximates the variation of $k(vj_{max} \rightarrow c;\ T)$ with v, and by definition has a minimal value of σ_0/σ_{HS} at $v = 0$ and a maximal value of unity at $v = v_{max}$.

Equations (16a) and (16b) provide two forms for $\varepsilon(v)$: the former is quadratic in v and the latter is exponential. These forms are motivated by the quasiclassical trajectory (QCT) calculations of Haug et al. who examined collisions of para-H_2 (p-H_2) with Ar. In their work, thermally averaged dissociative cross sections from specific (v, j) states were computed for $T = 4500$ K. We observed[13] an essentially quadratic variation of their dissociative cross sections with v. Specifically, we isolated those cross sections corresponding to dissociative transitions from the highest-lying bound (but not quasibound) vibrational-rotational states.

The calculations of Haug et al. yield $\sigma_0 = 0.0$ Å^2 for p-H_2–Ar collisions. We have arbitrarily chosen $\sigma_0 = 0.01$ Å^2 for our calculations because we encountered numerical difficulties for $\sigma_0 = 0.0$ Å^2. However, for $0.0001 < \sigma_0 < 0.1$ Å^2 our master equation calculations did not show significant quantitative differences.[13]

In Fig. 1 we show $\varepsilon_{quad}(v)$ and $\varepsilon_{exp}(v)$ for CO–Ar collisions. As will be discussed below, the quadratic form [Eq. (16a)] worked better for N_2 and O_2, and the exponential form [Eq. (16b)] worked better for CO.

Linear Kinetics

For highly dilute mixtures of diatomics in Ar, in which diatom-diatom collisions and back reactions are neglected,

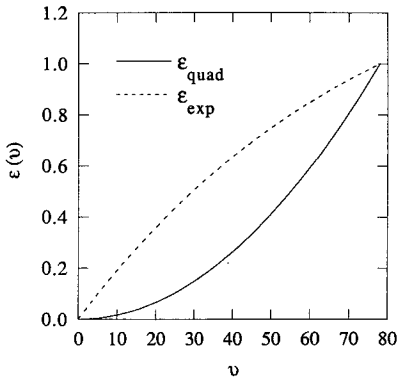

Fig. 1 Quadratic and exponential bridging functions for CO–Ar collisions.

the master equation is linear in the molecular fractional populations X_v

$$\frac{dX_v}{dt} = \sum_{v' \neq v}[\tilde{k}_{v'v}X_{v'} - \tilde{k}_{vv'}X_v] - \tilde{k}_{vc}X_v \quad (17)$$

where

$$X_v(t) = \frac{n_v(t)}{\sum_v n_v(0)} = \frac{n_v(t)}{n(0)} \quad (18)$$

and where the summations are over all bound vibrational levels of the diatom. The pseudo-first-order rate coefficients are given by $\tilde{k}_{vv'} = k(v \rightarrow v';\ T)\rho$ and $\tilde{k}_{vc} = k(v \rightarrow c;\ T)\rho$. Here, $n_v(t)$ is the number density of diatomic molecules at time t, and ρ is the number density of the argon diluent. To compare directly with other studies, we take ρ to be 1.28×10^{17} molecules cm^{-3}. It should be noted that the distribution $X_v(t)$ is normalized to unity only at $t = 0$. Equation (17) can be written more compactly as

$$\frac{dX_v}{dt} = \sum_{v'} K_{vv'}X_{v'} \quad (19)$$

where $K_{vv'}$ are elements of the rate matrix K

$$K_{vv'} = \tilde{k}_{v'v}, \qquad v' \neq v \quad (20)$$

$$K_{vv} = -\sum_{v' \neq v}\tilde{k}_{vv'} - \tilde{k}_{vc} \quad (21)$$

The general solution to Eq. (19) is

$$X_v(t) = \sum_m a_m u_{vm} \exp(\omega_m t) \quad (22)$$

where ω_m and u_{vm} are the eigenvalues and normalized eigenvectors, respectively, of the rate matrix K, i.e., $Ku_m = \omega_m u_m$ with $\omega_m < 0$ for all m. The eigenvectors are normalized according to $\Sigma_v u_{vm} = 1$. The constants of integration a_m are determined from the initial condition, which we always take to be a normalized Boltzmann distribution at the initial temperature T_i.

If $|\omega_1|$ is the eigenvalue of smallest absolute value and $|\omega_2|$ is the next smallest, then for $t >> (|\omega_2| - |\omega_1|)^{-1}$ the steady-state distribution is[15]

$$X_v^{ss} = a_1 u_{v1} \exp(\omega_1 t) \quad (23)$$

and the normalized steady-state distribution is

$$P_v^{ss} = X_v^{ss}/\sum_v X_v^{ss} = u_{v1} \quad (24)$$

The steady-state distribution is obtained at long times when all eigenmodes, except the one corresponding to ω_1, have decayed and no longer contribute to the sum in Eq. (22). P_v^{ss} is simply the normalized eigenvector corresponding to ω_1.

The induction time is defined as[16]

$$t_i = |\omega_1|^{-1} \text{ if } a_1 \tag{25}$$

and the average dissociative rate coefficient at steady state is given by

$$k_d^{ss}(T) = \sum_v P_v^{ss} k(v \rightarrow c; T) \tag{26}$$

Results

Evaluation of Inelastic Rate Coefficients

In this section we compare inelastic rate coefficients computed by information theory (IT) with those computed by the method of Schwartz et al.[17] commonly known as SSH theory. In particular, we consider the Keck and Carrier version[18] of SSH theory which has been used recently in master equation studies.[3,4] The SSH rate coefficients are given by[3,4]

$$k_{SSH}(v \rightarrow v'; T) = sZw(v \rightarrow v'; T) \tag{27}$$

where

$$w(v \rightarrow v'; T) = U_{vv'}^2 \left(\frac{32\pi^2\mu\kappa T}{\alpha^2 h^2}\right) f(\xi) \tag{28}$$

$$f(\xi) = 0.5[3 - \exp(-2\xi/3)]\exp(-2\xi/3), \quad 0 \le \xi \le 21.622 \tag{29a}$$

$$f(\xi) = 8(\pi/3)^{1/2}\xi^{7/3}\exp(-3\xi^{2/3}), \quad \xi > 21.622 \tag{29b}$$

$$\xi = \left(\frac{2\pi^4\mu(\Delta E)^2}{\alpha^2 h^2 \kappa T}\right)^{1/2} \tag{30}$$

and $\Delta E = E_{v'} - E_v$. Here, $w(v \rightarrow v'; T)$ is the thermal probability for the $v \rightarrow v'$ transition, s is the steric factor, $U_{vv'}$ is the matrix element for the $v \rightarrow v'$ transition, α is the inverse range parameter, and h is Planck's constant. We take $s = \frac{1}{3}$ and obtain the value of α from Ref. 19.

We scale the SSH rates so that they reproduce the $1 \rightarrow 0$ result in the harmonic oscillator/Landau-Teller approximation, given by

$$k_{HO}(1 \rightarrow 0; T) = \{(p\tau)\beta[1 - \exp(-\theta/T)]\}^{-1} \tag{31}$$

where θ is the characteristic vibrational temperature for the diatom. The scaling term η is defined by

$$\eta = \frac{k_{HO}(1 \rightarrow 0; T)}{k_{SSH}(1 \rightarrow 0; T)} \tag{32}$$

The set of scaled SSH rates are thus obtained by the relation

$$k_{SSH}^{sc}(v \rightarrow v'; T) = \eta k_{SSH}(v \rightarrow v'; T) \tag{33}$$

This set of rate coefficients is designated SSH/sc. Similar scaling techniques were used in Refs. 3 and 4.

We are aware of no published high-temperature state-to-state cross sections or rate coefficients, either computed or measured, for Ar collisions with CO, N_2, or O_2. Therefore, our comparisons with the SSH/sc results are only qualitative. However, we can compare the IT and SSH/sc rates with the QCT calculations of Duff et al.[20] who computed thermally averaged state-to-state cross sections $\sigma_{QCT}(v \rightarrow v'; T)$ for p-H_2–Ar collisions at 4500 K.

As shown in Ref. 20, rate coefficients may be computed from thermal QCT cross sections according to

$$k_{QCT}(v \rightarrow v'; T) = \langle v \rangle_v \sigma_{QCT}(v \rightarrow v'; T) \tag{34}$$

where the thermal cross sections are defined by

$$\sigma_{QCT}(v \rightarrow v'; T) = \frac{\sum_{j'} \langle\langle v\sigma_{QCT}(vj \rightarrow v'j'; v)\rangle_j\rangle_v}{\langle v \rangle_v} \tag{35}$$

Here, $\langle\ \rangle_j$ denotes a Boltzmann average over initial j states, $\langle\ \rangle_v$ denotes a Maxwellian average over relative collision velocities v at the temperature T, and $\langle v \rangle_v = (8\kappa T/\pi\mu)^{1/2}$. Thus, normalized QCT rate coefficients are given by

$$k_{QCT}(v \rightarrow v'; T)/Z = \sigma_{QCT}(v \rightarrow v'; T)/\sigma_{HS} \tag{36}$$

For p-H_2–Ar, $k_{HO}(1 \rightarrow 0; T) = 1.38 \times 10^{-12}$ cm^3 molecule^{-1} s^{-1}, and the corresponding IT value is 1.1×10^{-12} cm^3 molecule^{-1} s^{-1}. This good agreement is expected since the IT rates are essentially scaled by $(p\tau)$. We computed a value of 4.4×10^{-11} cm^3 molecule^{-1} s^{-1} for $k_{QCT}(1 \rightarrow 0; T)$ using $k_{QCT}(0 \rightarrow 1; T)$ provided in Ref. 20 and detailed balance. The QCT value is larger than the IT value by a factor of 40. We will assume that $k_{QCT}(1 \rightarrow 0; T)$ is accurate, and thus scale all the IT rates by this factor. For consistency, we use $k_{QCT}(1 \rightarrow 0; T)$ instead of $k_{HO}(1 \rightarrow 0; T)$ to scale the SSH/sc rate coefficients.

In Figs. 2a and 2b we show normalized rate coefficients $k(v \rightarrow v'; T)/Z$ for transitions from the initial states $v = 4$ and $v = 10$, respectively, for the p-H_2–Ar case. For the SSH/sc calculations, we use $\alpha = 1.72a_0^{-1}$ (3.25 Å^{-1}) as given in Ref. 20, where a_0 is the Bohr radius, and we compute $\eta = 0.637$. Duff et al.[20] determined this value for α using the same potential energy surface as in their QCT calculations. The figures show that the IT rates provide better matching to the QCT results for all initial and final vibrational states presented. In general, one observes large differences between the SSH/sc and QCT rates, especially for multiquantum transitions. In

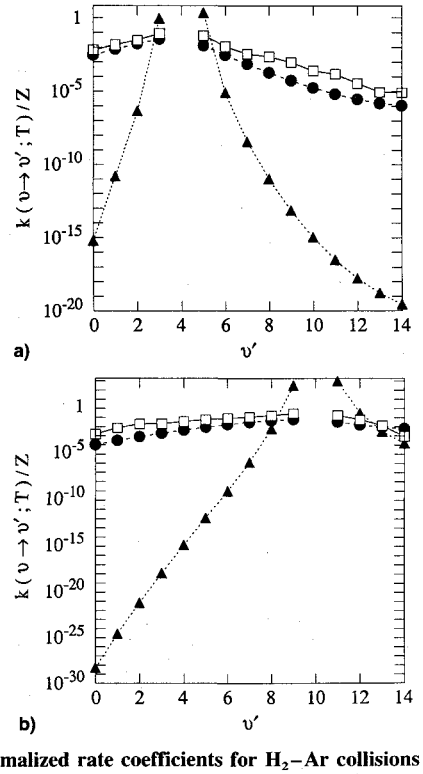

Fig. 2 Normalized rate coefficients for H_2–Ar collisions at 4500 K. QCT[20] (squares), scaled IT (circles), rescaled SSH/sc (triangles): a) $v = 4$ and b) $v = 10$.

Fig. 2a, the SSH/sc method provides reasonable accuracy only for nearest neighbor transitions. However, in Fig. 2b one can see that the nearest neighbor SSH/sc rates exceed the hard sphere rate Z by 2 orders of magnitude.

It should be mentioned that the sum rule [Eq. (13a)] is linear in the vibrational energy E_v [Eq. (13b)], and is a necessary and sufficient condition for exponential relaxation of the average vibrational energy to equilibrium.[8] Truhlar and Blais[21] have tested the validity of the linear sum rule assumption by computing Eq. (13a) for p-H_2–Ar collisions at 4500 K using QCT rate coefficients derived from a realistic potential energy surface. The rate coefficient for vibrational relaxation $k_{\text{relax}}(T) \equiv \kappa T/(p\tau)$, computed by taking the ratio $\Gamma(v; T)/[V(\infty) - E_v]$, was found to be v-dependent. Specifically, $k_{\text{relax}}(T)$ varied at most by a factor of 5.5 over the range $0 \leq v \leq 13$. Thus, they concluded that a surprisal synthesis based on the sum rule of Eq. (13) would be an inaccurate means to compute $k(v \rightarrow v'; T)$.

Moreover, we have shown elsewhere[13] that the unscaled IT rate coefficients for p-H_2–AR collisions at 4500 K underpredict the QCT values of Duff et al.[20] by more than 2 orders of magnitude. A least squares fit to the Duff et al. values resulted in a scaling factor of 152 for the IT rate coefficients. QCT (or other sophisticated) calculations of other diatomic systems would be useful to further examine the validity of the sum rule.

Despite these problems, the good agreement between the scaled IT and QCT results suggests that if one knows the value of only one QCT rate coefficient, then an entire set of reasonably accurate state-to-state IT rate coefficients may be efficiently obtained. While we have shown that this is the case for p-H_2–Ar, an extrapolation of this observation to other diatomics awaits corresponding detailed computational chemistry calculations with which to compare.

Since N_2 has been the subject of many recent investigations,[1-6] we compare in Fig. 3 the (unscaled) IT rates with the SSH/sc rates [Eq. (33)] for transitions from the initial states $v = 15$ and $v = 50$, respectively, for N_2–Ar collisions. We compute $\eta = 15.3$, and again see large differences between the IT and SSH/sc rates for multiquantum transitions.

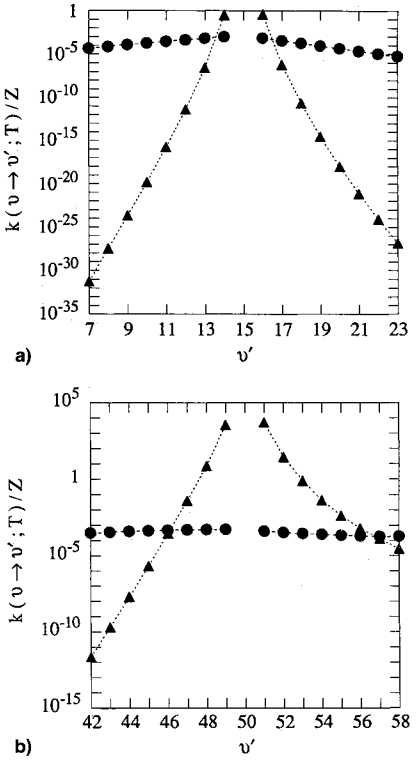

Fig. 3 Normalized rate coefficients for N_2–Ar collisions at 8000 K. IT (circles), SSH/sc (triangles): a) $v = 15$ and b) $v = 50$.

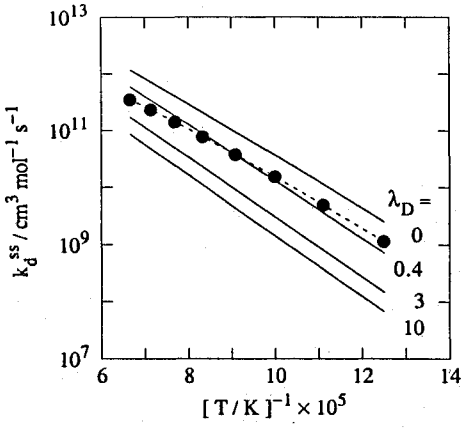

Fig. 4 Steady-state dissociative rate coefficients for CO in Ar. Computations (solid lines), experimental data[22] (circles).

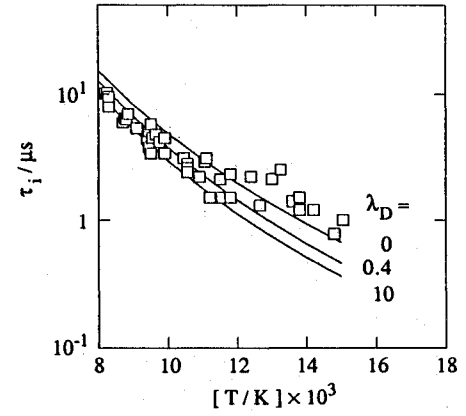

Fig. 5 Induction times for dissociation of CO in Ar. Computations (solid lines), experimental data[22] (squares).

In addition, as in the H_2–Ar case, some SSH/sc rates exceed Z for large v. For $v = 50$, we see that the IT and SSH/sc rates are closest for multiquantum transitions. This behavior suggests that the scaling parameter η, while allowing good matching for the $1 \rightarrow 0$ transition, causes (perhaps unphysical) overpredictions of nearest neighbor (and sometimes higher) transitions from high v states.

In the absence of sophisticated computational chemistry calculations or experimental measurements for CO, N_2, and O_2, we assume that the IT inelastic rates are reasonable for engineering purposes and use them in all remaining calculations in this work.

Determination of λ_D

To determine λ_D, we first compute the average steady-state dissociative rate coefficient $k_d^{ss}(T)$ and the induction time t_i and then select the value of λ_D which best fits the corresponding shock tube data. In Figs. 4 and 5 we plot $k_d^{ss}(T)$ and t_i for several values of λ_D for the CO–Ar case over the temperature range $8000 \leq T \leq 15{,}000$ K and $T_i = 300$ K and compare with the shock tube data of Ref. 22. The best matching occurs for $\lambda_D \approx 0.4$. For N_2 and O_2 (not shown), the best matching occurs for $\lambda_D \approx 1$.

As expected, the $k_d^{ss}(T)$ curves shift downward with increasing λ_D for each molecular species. This is because λ_D acts as a biasing parameter that effectively reduces the number of (v, j) states from which dissociation may occur as it increases. In addition, for a given λ_D, the $k_d^{ss}(T)$ curves have higher absolute value when the exponential bridging function is used instead of the quadratic one. This is due to the relatively larger dissociative cross sections in the exponential bridging function model (Fig. 1). As mentioned earlier, $\varepsilon_{\text{exp}}(v)$ worked better for CO because $\varepsilon_{\text{quad}}(v)$ resulted in curves that were below the experimental data for all λ_D.

Steady-State and Transient Results

The fractional contribution of each vibrational state to the average steady-state dissociative rate coefficient is given by

$$f_v^{ss} = P_v^{ss} k(v \rightarrow c;\ T)/k_d^{ss}(T) \qquad (37)$$

In Fig. 6, we show f_v^{ss} for CO–Ar at the heat bath temperatures T = 8000, 12,000, and 15,000 K, and the initial temperature T_i = 300 K. It can be seen that the majority of the contribution to $k_d^{ss}(T)$ comes from low- and midlying vibrational levels with the contribution from high-lying states increasing with increasing temperature. The peak contribution is near v = 20. Similar behavior was observed for N_2 and O_2.

We next consider the relative contribution of each vibrational state to $k_d^{ss}(T)$ by measuring its distance from the dissociation threshold (DT) in units of κT. Many simple theories assume that only those vibrational states which are within a few κT of the DT contribute significantly to dissociation. Figures 7a and 7b are linear plots of f_v^{ss} vs E_v/D_0 for CO at 8000 and 15,000 K, respectively. On the upper axis we show $(D_0 - E_v)/\kappa T$. [The irregularities in the curves are a result of rotational averaging in the calculation of $k(v \rightarrow c;\ T)$.] The figures indicate that most dissociation occurs from vibrational states that are many κT below the DT. This behavior is due to the contribution of rotational energy to dissociation. Similar results can be seen for N_2 and O_2, and these are shown in Figs. 7c and 7d for T = 8000 K, respectively.

It should be noted that for high enough temperatures, $D_0/\kappa T$ is so small that *all* vibrational levels are within a few κT of the DT (Figs. 7a and 7b illustrate this trend). Therefore, at high temperatures the number of κT below the DT is not a meaningful measure of internal state contribution to dissociation. In addition, at a given temperature $(D_0 - E_v)/\kappa T$ is smaller for molecules with relatively lower D_0. This can be observed in Figs. 7a, 7c, and 7d for which $D_0^{CO} > D_0^{N_2} > D_0^{O_2}$.

The results in Figs. 6 and 7 contradict the notion that the overall dissociative rate coefficient is biased to high-lying vibrational states. Itoh et al.[23] and Haug et al.[15] have shown that this is not the case. Itoh et al. solved the vibrational master equation for shock-heated Br_2–Ar and Br_2–Br mixtures using rate coefficients derived from QCT calculations. They concluded that the dominant contribution to $k_d^{ss}(T)$ comes from low v and high j states. Haug et al. examined shock-heated p-H_2–Ar. They solved a vibrational-rotational master equation and demonstrated that the most significant contribution to $k_d^{ss}(T)$ comes from mid v and high j states. Thus, our relatively simpler model qualitatively reproduces these more elaborate calculations. In addition, Blais and Truhlar[24] have shown for p-H_2–Ar collisions that states which lie near the dissociation threshold [i.e., high (v, j)] have relatively higher state-specific dissociative cross sections, and therefore, relatively higher rate coefficients $k(v \rightarrow c;\ T)$. Their results confirm the more accurate notion that state-specific dissociative rate coefficients are biased to high-lying internal states. Therefore, we observe a distinction between the state-specific

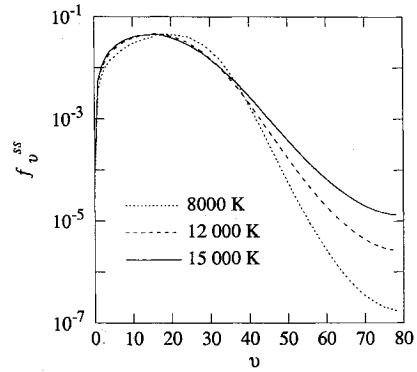

Fig. 6 Logarithmic plot of the relative contribution of vibrational states to the average steady-state dissociative rate coefficient for CO in Ar.

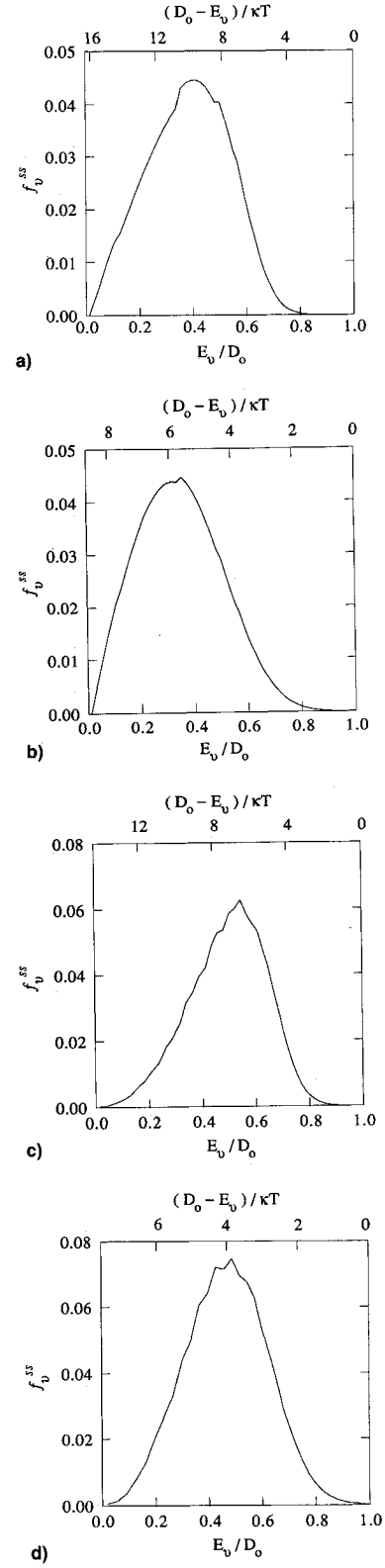

Fig. 7 Linear plots of the relative contribution of vibrational states to the average steady-state dissociative rate coefficient: a) CO–Ar collisions at 8000 K, b) CO–Ar collisions at 15,000 K, c) N_2–Ar collisions at 8000 K, and d) O_2–Ar collisions at 8000 K.

dissociative rate coefficients $k(v \rightarrow c;\ T)$ and the overall rate coefficient $k_d^{ss}(T)$, which is a weighted sum of the state-specific rate coefficients [see Eq. (26)].

A measure of nonequilibrium effects at steady state is given by the variable $\gamma(T)$, defined as

$$\gamma(T) \equiv k_d^{ss}(T)/k_d^{eq}(T) \qquad (38)$$

$$k_d^{eq}(T) = \sum_v P_v^{eq} k(v \rightarrow c;\ T) \qquad (39)$$

where $k_d^{eq}(T)$ is the average dissociative rate coefficient at equilibrium, and P_v^{eq} is the normalized equilibrium population in vibrational level v. This ratio was considered by Haug et al.[15] for p-H_2–Ar collisions at 4500 K and was described as a correction factor for nonequilibrium. They computed $\gamma(T) = 1/2.8 \approx 0.36$. In Fig. 8 we show $\gamma(T)$ for CO–Ar and N_2–Ar collisions over the range $8000 \leq T \leq 15{,}000$ K, and for O_2–Ar collisions over the range $2500 \leq T \leq 12{,}000$ K. [These temperature ranges are consistent with the experimental data that were used to determine the respective values for λ_D: CO (Ref. 22), N_2 (Ref. 25), O_2 (Ref. 26)]. For each case, the initial temperature $T_i = 300$ K. It can be seen that nonequilibrium effects are significant over the range of temperatures shown, especially for N_2–Ar and O_2–Ar collisions. The relative position of the curves for the given species is as expected since O_2 is the most easily dissociated, while CO is the most difficult. In addition, an interesting trend is observed that appears to be consistent with the bond strength of the diatom: at some value of T, $\gamma(T)$ increases. This indicates that at temperatures higher than some critical temperature T_c^i, where the superscript i denotes the diatomic species, $k_d^{ss}(T)$ increases faster than $k_d^{eq}(T)$ with increasing T. It is evident from Fig. 8 that values for T_c^i appear in the order of increasing D_0, i.e., the lowest value is observed for O_2, then N_2, and the highest value is expected to be observed for CO at some temperature above 15,000 K.

Figure 9 shows the time evolution of the normalized populations $P_v(t)$ for CO–Ar. The initial and final temperatures are 4000 and 15,000 K, respectively. The normalized populations may be inferred from Eq. (24) as $P_v(t) = X_v(t)/\Sigma_v X_v(t)$. The solid lines labeled P_v^i and P_v^f represent the initial and final Boltzmann distributions. Since recombination reactions are not included in this study, the P_v^f distribution is never obtained. One observes that the CO–Ar system relaxes uniformly to the steady-state distribution, labeled ss. We identify the steady-state time by $\tau_{ss} = |\omega_1|^{-1} = 8.2\ \mu$s. The distribution labeled a represents the distribution at the earliest time we show, namely $t = 10^{-4}\tau_{ss}$. Succeeding distributions are at 10^{-3}, 10^{-2}, . . . , τ_{ss}. The distributions show slight overpopulations of the high-lying states at the earliest times and underpopulations at the latest times. The distributions at steady state and at $10^{-1}\tau_{ss}$ are nearly coincident. Similar results were obtained for N_2 and O_2. The overpopulation of high v states at early times has been attributed to the strong influence of multiquantum transitions.[27]

The distributions presented in Fig. 9 were computed on a Cray Y-MP using the EISPACK subroutine RG,[28] and required approximately 5 CPU s.

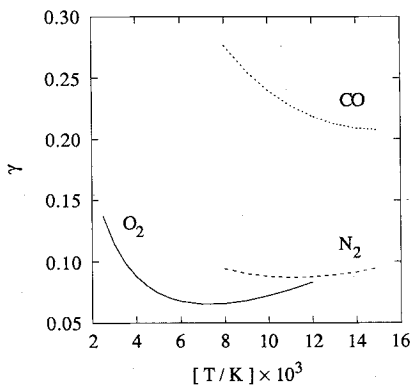

Fig. 8 Ratio of the steady-state dissociative rate coefficient to the equilibrium value for CO, N_2, and O_2 in Ar.

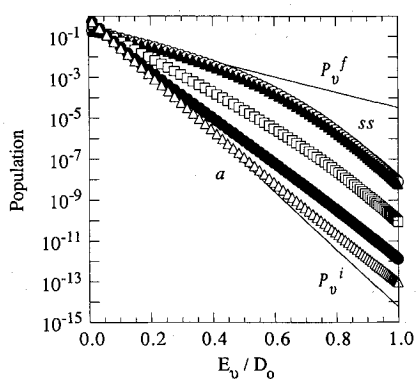

Fig. 9 Time evolution of the normalized vibrational populations during dissociation of CO in Ar. See text for definition of labels.

Single vs Multiquantum Effects

Finally, we consider the effect of single and multiquantum transitions on overall (bulk) observables in the shock-heated gas mixture. The two observables we compute are the average vibrational energy $V(t)$ and the average dissociative rate coefficient $k_d(t)$, given by

$$V(t) = \sum_v P_v(t) E_v \qquad (40)$$

$$k_d(t) = \sum_v P_v(t) k(v \rightarrow c;\ T) \qquad (41)$$

$V(t)$ and $k_d(t)$ are the variables one would compute in nonequilibrium flow codes.

In Figs. 10a and 10b we calculate $V(t)$ and $k_d(t)$, respectively, in two ways: first, we allow all inelastic transitions, both nearest neighbor and multiquantum; and second, we allow only nearest neighbor inelastic transitions. We use IT rate coefficients for all inelastic transitions. We consider a highly dilute mixture of O_2 in Ar that is shock-heated from 2000 to 10,000 K. One can see in Fig. 10 that if only nearest neighbor transitions are allowed, the $V(t)$ and $k_d(t)$ profiles are shifted to longer times and lower absolute values. The

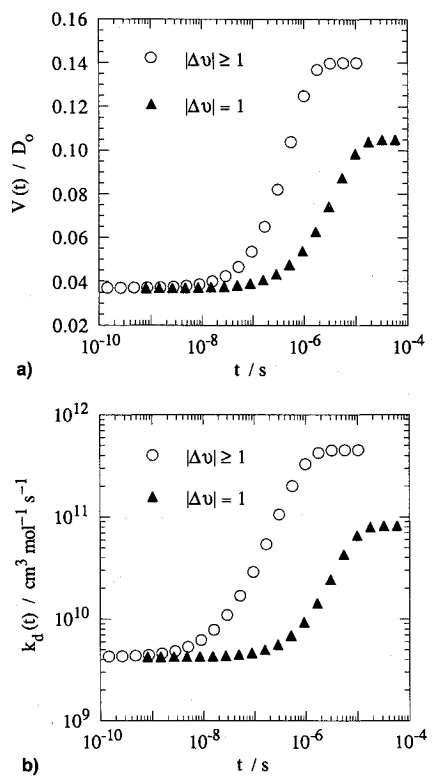

Fig. 10 Time evolution of the average vibrational energy of O_2 in a) Ar computed using nearest neighbor (only) and multiquantum IT inelastic rate coefficients. b) Same as in a) except for the average dissociative rate coefficient.

time shift is an indication that multiquantum transitions increase the rate at which high-lying states are populated. Near 1 μs, the nearest neighbor result underpredicts the multiquantum result by ~60% for $V(t)$ and by a factor of ~30 for $k_d(t)$. At steady state, the nearest neighbor value underpredicts by ~30% for $V(t)$ and by a factor of ~5 for $k_d(t)$. Thus, we observe that $k_d(t)$ is more sensitive than $V(t)$ to the effect of multiquantum transitions.

Conclusions

In this article we show that information theoretic rate coefficients compare well with published quasiclassical trajectory calculations for p-H_2–Ar collisions after appropriate scaling by a single factor. We also compare information theoretic rate coefficients with rate coefficients determined from the theory of SSH for p-H_2–Ar and N_2–Ar collisions and conclude that the information theoretic rates are superior to the SSH rates, especially for multiquantum transitions. In addition, information theoretic rate coefficients are well suited for engineering solutions of the master equation since an entire set of inelastic rate coefficients can be easily generated knowing only the internal energies and the product of the pressure and vibrational relaxation time.

Our master equation results indicate that at steady state the most significant contribution to the average dissociative rate coefficient comes from low- and mid-lying vibrational levels for shock-heated mixtures of CO, N_2, and O_2 highly dilute in Ar. This corresponds to a significant number of κT energy units below the dissociation threshold. We find, for a given initial temperature, that the contribution from high-lying states increases with increasing heat bath (final) temperature. In addition, it was shown that the steady-state dissociative rate coefficient is far from its equilibrium value for the temperatures considered in this study.

Finally, an examination of the effects of multiquantum transitions shows that omitting multiquantum transitions shifts the relaxation to steady state to longer times and results in large underpredictions of the average vibrational energy and the average dissociative rate coefficient.

Acknowledgments

This work was supported by NASA Minority Graduate Engineering Grant NGT-70032, the NASA Center for Hypersonic Research and Training Grant NAGW-964, and the Texas Advanced Research Program. Computing resources were provided by the University of Texas System Center for High Performance Computing.

References

[1]Sharma, S. P., Huo, W. M., and Park, C., "Rate Parameters for Coupled Vibration-Dissociation in a Generalized SSH Approximation," *Journal of Thermophysics and Heat Transfer*, Vol. 6, No. 1, 1992, pp. 9–21.

[2]Olynick, D., Moss, J., and Hassan, H., "Monte Carlo Simulation of Vibrational Relaxation in Nitrogen," *Journal of Thermophysics and Heat Transfer*, Vol. 6, No. 1, 1992, pp. 22–26.

[3]Landrum, D., and Candler, G., "Vibration-Dissociation Coupling in Nonequilibrium Flows," *Journal of Thermophysics and Heat Transfer*, Vol. 6, No. 4, 1992, pp. 643–649.

[4]Ruffin, S. M., and Park, C., "Vibrational Relaxation of Anharmonic Oscillators in Expanding Flows," AIAA Paper 92-0806, Jan. 1992.

[5]Gonzales, D. A., and Varghese, P. L., "Vibrational Relaxation and Dissociation in Nitrogen," AIAA Paper 91-1370, June 1991.

[6]Gonzales, D. A., and Varghese, P. L., "Rate Calculations for the Simultaneous Vibrational Relaxation and Dissociation of Nitrogen," AIAA Paper 92-0808, Jan. 1992.

[7]Gonzales, D. A., and Varghese, P. L., "Master Equation Calculations of Vibrational Non-Equilibrium and Dissociation Kinetics," *Proceedings of the Institut Universitaire Technologique d'Aix en Provence et Marseille (IUTAM) Symposium on Aerothermochemistry of Spacecraft and Associated Hypersonic Flows*, Marseille, France, 1992.

[8]Procaccia, I., and Levine, R. D., "Vibrational Energy Transfer in Molecular Collisions: An Information Theoretic Analysis and Synthesis," *Journal of Chemical Physics*, Vol. 63, No. 10, 1975, pp. 4261–4279.

[9]Levine, R. D., and Bernstein, R. B., "Thermodynamic Approach to Collision Processes," *Dynamics of Molecular Collisions, Part B*, edited by W. H. Miller, Plenum Press, New York, 1976, pp. 323–364.

[10]Huxley, P., and Murrell, J. N., "Ground-State Diatomic Potentials," *Journal of the Chemical Society, Faraday Transactions 2*, Vol. 79, 1983, pp. 323–328.

[11]Gonzales, D. A., and Varghese, P. L., "Vibration-Dissociation Coupling in CO, N_2 and O_2: An Evaluation of Analytic Transition Rate Expressions," AIAA Paper 93-0481, Jan. 1993.

[12]Millikan, R. C., and White, D. R., "Systematics of Vibrational Relaxation," *Journal of Chemical Physics*, Vol. 39, No. 12, 1963, pp. 3209–3213.

[13]Gonzales, D. A., and Varghese, P. L., "A Simple Model for State-Specific Diatomic Dissociation," *Journal of Physical Chemistry*, Vol. 97, No. 29, 1993, pp. 7612–7622.

[14]Bird, R. B., Stewart, W. E., and Lightfoot, E. N., *Transport Phenomena*, Wiley, New York, 1960, p. 744.

[15]Haug, K., Truhlar, D. G., and Blais, N. C., "Monte Carlo Trajectory and Master Equation Simulation of the Nonequilibrium Dissociation Rate Coefficient for Ar + H_2 → Ar + 2H at 4500 K," *Journal of Chemical Physics*, Vol. 86, No. 5, 1987, pp. 2697–2716.

[16]Kiefer, J. H., and Hajduk, J. C., "A Vibrational Bias Mechanism for Diatomic Dissociation: Induction Times and Steady Rates for O_2, H_2 and D_2 Dilute in Ar," *Chemical Physics*, Vol. 38, 1979, pp. 329–340 (the expression for t_i in this reference [their Eq. (4)] is in error).

[17]Schwartz, R. N., Slawsky, Z. J., and Herzfeld, K. F., "Calculation of Vibrational Relaxation Times in Gases," *Journal of Chemical Physics*, Vol. 20, No. 10, 1952, pp. 1591–1599.

[18]Keck, J., and Carrier, G., "Diffusion Theory of Nonequilibrium Dissociation and Recombination," *Journal of Chemical Physics*, Vol. 43, No. 7, 1965, pp. 2284–2298.

[19]Radzig, A. A., and Smirnov, B. M., *Reference Data on Atoms, Molecules, and Ions*, Springer Series in Chemical Physics 31, Springer-Verlag, Berlin, 1985, p. 315.

[20]Duff, J. W., Blais, N. C., and Truhlar, D. G., "Monte Carlo Trajectory Study of Ar + H_2 Collisions: Thermally Averaged Vibrational Transition Rates at 4500 °K," *Journal of Chemical Physics*, Vol. 71, No. 11, 1979, pp. 4304–4320.

[21]Truhlar, D. G., and Blais, N. C., "Test of the Linear Sum Rule for Vibrational Energy Transfer by Trajectory Calculations," *Journal of Chemical Physics*, Vol. 77, No. 5, 1982, pp. 2430, 2431.

[22]Appleton, J. P., Steinberg, M., and Liquornik, D. J., "Shock-Tube Study of Carbon Monoxide Dissociation Using Vacuum-Ultraviolet Absorption," *Journal of Chemical Physics*, Vol. 52, No. 5, 1970, pp. 2205–2221.

[23]Itoh, H., Koshi, M., Asaba, T., and Matsui, H., "Vibrational Nonequilibrium Dissociation of Br_2 in Collisions with Ar and Br Atoms," *Journal of Chemical Physics*, Vol. 82, No. 11, 1985, pp. 4911–4915.

[24]Blais, N. C., and Truhlar, D. G., "Monte Carlo Trajectory Study of Ar + H_2: Vibrational Selectivity of Dissociative Collisions at 4500 °K and the Characteristics of Dissociation Under Equilibrium Conditions," *Journal of Chemical Physics*, Vol. 70, No. 6, 1979, pp. 2962–2978.

[25]Appleton, J. P., Steinberg, M., and Liquornik, D., "Shock-Tube Study of Nitrogen Dissociation Using Vacuum-Ultraviolet Light Absorption," *Journal of Chemical Physics*, Vol. 48, No. 2, 1968, pp. 599–608.

[26]Breshears, W. D., Bird, P. F., and Kiefer, J. H., "Density Gradient Measurements of O_2 Dissociation in Shock Waves," *Journal of Chemical Physics*, Vol. 55, No. 8, 1971, pp. 4017–4026; Watt, W. S., and Myerson, A. L., "Atom Formation Rates Behind Shock Waves in Oxygen," *Journal of Chemical Physics*, Vol. 51, No. 4, 1969, pp. 1638–1643; Wray, K. L., "Shock-Tube Study of the Recombination of O Atoms by Ar Catalysts at High Temperatures," *Journal of Chemical Physics*, Vol. 38, No. 7, 1963, pp. 1518–1524; Wray, K. L., "Shock-Tube Study of the Coupling of the O_2–Ar Rates of Dissociation and Vibrational Relaxation," *Journal of Chemical Physics*, Vol. 37, No. 6, 1962, pp. 1254–1263.

[27]McElwain, D. L. S., and Pritchard, H. O., "The Temperature Coefficients of Diatomic Dissociation and Recombination Reactions," *Thirteenth Symposium (International) on Combustion*, Combustion Inst., Pittsburgh, PA, 1971, pp. 37–49.

[28]Smith, B. T., Boyle, J. M., Dongarra, J. J., Garbow, B. S., Ikebe, Y., Klema, N. C., and Moler, C. B., *Matrix Eigensystem Routines—EISPACK Guide*, Springer-Verlag, Berlin, 1976.